Journal of Structural Engineering and Geotechnics,
12(2), 75-89, Summer & Autumn 2022

A Numerical Study on the Seismic Performance of a RC-Bridge with Random Pier Scouring

Ali Raoof Mehrpour Hosseini [a], Mehran Seyed Razzaghi [a,*], Nasser Shamskia [a]

[a]*Department of Civil Engineering, Qazvin Branch, Islamic Azad University, Qazvin, Iran*

Received 15 September 2023, Accepted 18 October 2023

Abstract

A multi-hazard investigation approach is a vital requirement for a realistic risk assessment of infrastructures. The combined impact of scouring and earthquake can result in a distinctive effect on the performance of a given bridge. Scouring, being a hazard influenced by various factors, entails numerous uncertainties. Several prior investigations have explored the multi-hazard of scour-earthquake; however, the associated implementation has not accounted for the random scour depths around the foundations of differing bents. This study provides a probabilistic platform to investigate the effect of random scouring on the seismic performance of a multi-span RC bridge. In this regard, researchers employed Monte Carlo simulation to develop a probability hazard curve for scour. The Latin Hypercube technique was applied to randomly select depths, enabling the generation of non-uniform patterns for the depth of cavities formed in different foundations. Subsequently, the study involved conducting non-linear time history analyses on the finite element model. The uniform scouring patterns were also examined to compare the models. The scouring around foundations significantly affects the responses of bridge elements, as it influences the total base shear of the structure and the pounding forces between the superstructure elements.

Keywords: Bridge; Seismic evaluation; Scour; Multi-hazard; Performance assessment.

1-Introduction

Scouring at the foundation of bridges constructed in rivers, as a hydraulic failure, has been responsible for numerous incidents of bridge damage in recent decades [1-5]. Wardhana and Hadipriono [6] conducted a study of 500 bridge structure failures that occurred between 1989 and 2000. The ages of the bridges ranged from 1 to 157 years old. The study showed that flood and scour were the major causes for around 53% of the failures, making it the most frequent cause of bridge failures.
Prior investigations have monitored and analyzed the mechanics of scouring using various tools and instrumentation in laboratory and field settings [7-9]. The studies have discovered that scouring is unavoidable in the cases that are being investigated. Due to the difficulty and cost of monitoring river bridges, modern codes now emphasize accounting for scouring as a potential hazard in bridge design and retrofitting [10].

Several studies have proposed the addition of a load factor to account for scouring, in conjunction with other hazards [11]. Earthquake is one of several hazards that can pose significant threats to bridges, particularly in regions with high seismic activity.

Observational assessments of bridge damage following earthquakes have recorded instances of minor component damage as well as complete bridge collapse resulting from this hazard [12-15]. Therefore, in past decades, numerous studies have been conducted to evaluate the performance of bridge models under seismic loads, considering various conditions [16-18].

In recent years, several studies have been conducted to assess how multiple hazards affect bridge analysis. Most of these hazards have been linked with scouring, which holds a high probability of causing failures. Kameshwar and Padgett [19] evaluated the responses of columns and developed fragility curves for bridges that experienced barge-bridge collision and scouring. Hung and Yau [20] analyzed the behavior of scoured bridges subjected

*Corresponding Author: Email Address:razzaghi.m@gmail.com

to flood-induced loads. Of all multiple hazard assessments, it is worth noting that evaluating the combined effects of the earthquake and the scour holds significant importance. On one hand, the scouring can lead to reduced foundation support, and on the other hand, it can alter the structure's dynamic characteristics by decreasing its stiffness [21]. As a result, scouring can significantly affect the seismic response of the bridge. Therefore, the simultaneous impact of these two hazards has attracted considerable attention among researchers [22-26]. Employing static push-over analysis, He et al. [27] evaluated the seismic performance of a uniformly scoured four-span continuous model. They reported that the maximum base shear increased with the scour depth in dense sand, while it decreased in loose sand when the scour depth exceeded 8 meters.

The effect of uniform scouring on the seismic performance of a finite element model of the Sankata Bridge was evaluated by Shreshta et al. [28]. The results revealed that the pounding forces between the superstructure elements increased with the increase in the scouring depth for two hazard levels of design basis earthquake and maximum credible earthquake. However, the intact model did not exhibit any pounding.

Although several prior studies have explored the performance and vulnerability of scoured bridges under seismic analyses, certain drawbacks and research gaps remain. Previous studies mainly focused on evaluating multi-bent bridges with uniform scour depths among all foundations. In some cases, single-bent bridges with maximum credible scour depth were also assessed. In current literature, there is a noticeable lack of investigation regarding the seismic effects on bridges that exhibit non-uniform scouring patterns. Fioklou and Alipour [29] investigated the combined impact of earthquake and non-uniform scour by modeling the non-uniformity between piles of a single-bent bridge. The findings indicated that the maximum responses did not always occur at the uniform depths of scouring.

This study's primary aim is to investigate the random distribution of scour depth among the foundations of a multi-bent bridge model. In order to achieve this objective, this research employed Monte Carlo simulation to extract the probabilistic hazard curve of scour for the 100-year return period. Using this tool, researchers extracted samples that enabled the generation of 'uniform' and 'non-uniform' random patterns via the Latin Hypercube technique. A previous study on the fragility analysis of this model revealed that the probability of exceeding the limit states and the probability of pounding between the superstructure elements increased with the generation of different scouring scenarios [30]. This study has investigated the responses of distinct components under various scour scenarios.

2-Probabilistic Prediction of Scour Depth

One of the primary stages in investigations assessing the impact of scour on the performance of a structure entails appraising the scour potential at the site of the analyzed case. The reduction in foundation capacity caused by more critical depths of scouring can have significant implications on the overall structural stability of the bridge. Numerous prior studies have estimated the depth of scouring that occurs at the substructure of bridges situated in channels or riverbeds because of the action of flowing water [31-40]. The equations utilized for this purpose may contain a considerable quantity of input parameters, depending on factors such as the stream flow characteristics, the geometrical properties of bridge components, and the features of riverbed materials. As such, the computational analysis of these models can be subject to uncertainty due to the nature of these complex variables. Hence, several investigations have suggested adopting a probabilistic framework to carry out calculations concerning the evaluation of scour depth [41-43]. The utilization of these methods enables the derivation of probabilistic functions that express the probability of exceeding specified scour depth values.

As one of the primary aims of this investigation is to establish a random framework for simulating scour depth across various bents of the bridge model, it is imperative to employ a probability-based approach when estimating the depth of scour. Therefore, in this study, probabilistic assessments were performed using the correlation proposed by Johnson and Dock [41]. Several prior investigations have utilized this equation for modeling bridge scour on a probabilistic platform [11,44]. This equation denotes as follows:

$$y_s = 2.0\lambda_{sc} y_0 K_{sh} K_\theta K_3 K_4 \left(\frac{d_p}{y_0}\right)^{0.65} {F_r}^{0.43} \quad (1)$$

In this formula, variable y_s represents the depth of scour, while the variables K_{sh}, K_θ, K_3 and K_4 signify correction factors that adjust for the shape of

the pier, the flow's angle of attack, the condition of the stream bed, and the size of the bed material, respectively. Furthermore, the scour modeling correction factor is denoted by λ_{sc}, the pier diameter is represented by d_p, and the flow depth just upstream of the pier is denoted by y_0. Additionally, the equation involves the Froude number (F_r), which is expressed as:

$$F_r = \frac{V}{(gy_0)^{0.5}} \quad (2)$$

Where g is the gravitational acceleration, and V is the mean flow velocity which can be calculated as follow:

$$V = \frac{Q}{by_0} \quad (3)$$

$$Q = \frac{by_0}{n}\left(\frac{by_0}{b+2y_0}\right)^{0.67}S^{0.5} \quad (4)$$

In the equations above, Q is the discharge rate, b is the river width, and n is the Manning roughness coefficient.

Table 1 presents the suggested probability distributions to account for uncertainties associated with parameters in probabilistic scour depth prediction.

Table 1
Definition of random input variables for the probabilistic scour estimation [11,41,44].

Random Variable	Mean	COV.	Distribution Function
K_θ	1	0.05	Normal
K_3	1.1	0.05	Normal
n	0.025	0.275	Lognormal
λ_{sc}	0.93	N/A	Triangular*

* The boundaries of the triangular distribution are 0.8 and 1

Due to the lack of a currently established reliable probability distribution for K_{sh} and K_4, the variables are employed deterministically within the equation [11,41]. The correction factor K_{sh} is assigned a value of 1.0, for substructure elements with circular sections. The stream bed consists of medium sand. Therefore, in this study, a value of 1.0 was assigned to the correction factor K_4 - which accounts for larger particles in armored riverbeds - in the equation being used. The river width 'b' was assumed to be equal to the length of the bridge. Additionally, the slope value 'S' was taken as 0.002, which represents a relatively gentle slope [11]. The annual peak discharge data of a river in Iran was adopted from the Iran Water Resources Management Company and is shown in Fig. 1.

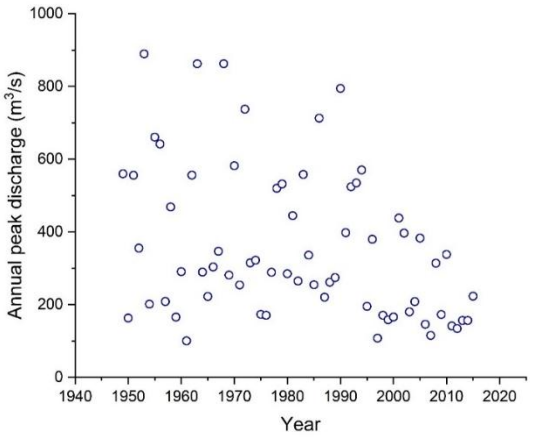

Fig. 1. The peak annual flow discharge of the river

In this study, to generate the hazard curve for scour, by utilizing the Monte Carlo simulation technique to take into account the parameters of probabilistic distributions along with other determined parameters in equation 1, a total of 100,000 simulations were carried out. It should be emphasized that the hazard curve was assessed for a return period of 100- years of flood events to adhere to design criteria outlined in specifications such as AASHTO [10]. A chi-squared goodness-of-fit test at the 5% significance level showed that the scour depth yielded a lognormal probability distribution. Fig. 2 illustrates the calculated hazard curve of the scour depth.

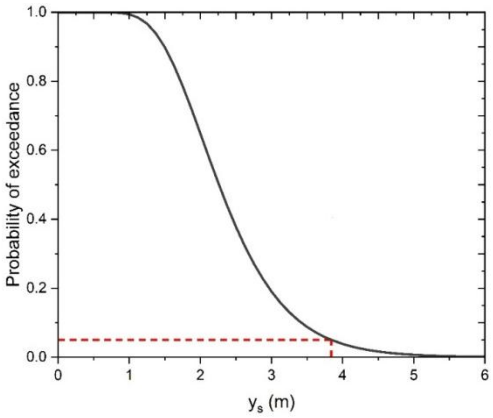

Fig. 2. Scour hazard curve for the bridge according to the river discharge rate

Given the lack of clear and widely agreed-upon procedures for identifying insignificant values of scour depth on the hazard curve, this study defines values below 5% on the scour hazard function as negligible. According to the details provided in Fig. 2, a scour depth equal to 3.84 meters is associated with a probability of 5% on the cumulative distribution curve. As a result, this study employs a value equivalent to 4 meters as the maximum credible scour depth.

Due to the significant number of samples generated through the Monte Carlo technique, it is nearly impossible to create different scour scenarios. Therefore, this study employed the Latin Hypercube sampling technique to produce samples based on the probability intervals of the scour hazard curve. This method assigns scour samples to different bents, creating patterns that may exhibit the same scour depth at distinct piers or uneven scour depths.

3- Case Study

3.1. Bridge Description

The present study aims to investigate a simply-supported multi-span RC bridge comprising a discontinuous deck-girder system that rests on bent caps via elastomeric bearing pads for support. It is worth mentioning that the bridge under investigation in this study is adopted from Mosleh et al. [45]. The bridge has a constant width of 11.95 m and an overall length of 79.2 m, consisting of four individual spans, with lengths of 15.6 m, 24 m, 24m, and 15.6 m, respectively. Each bent of the bridge is made up of three circular columns with a diameter of 1.1 m and a height of 6 m. The columns are reinforced with thirty 22 mm longitudinal steel bars which are confined by 12 mm spiral hoops spaced 250 mm apart. The specific compressive strength of concrete is 28 MPa in girders and 24 MPa in other elements. The bridge deck and abutments have a 50 mm gap, while adjacent deck segments have a 100 mm gap width. The foundation of each bent consists of six 1.2 m diameter, 20 m long piles with an integrated pile cap, which are reinforced with forty 22 mm diameter longitudinal bars.

3.2. Modeling

Nonlinear dynamic analyses were conducted on the bridge model using the OpenSees software [46] to assess the impact of earthquake loads on various scour scenarios in the bridge foundation. To capture the nonlinear responses of columns and piles subjected to scouring, these elements were modeled as displacement beam-column elements with fiber sections, whereas the superstructure elements, including deck and girders, were defined using equivalent elastic beam-column elements. The length of each pile was discretized into 0.25 m elements. The columns were also discretized into 0.25 m segments at the top and bottom and 0.5 m segments at the middle. The displacement beam-column elements used in the modeling were composed of confined and unconfined concrete, along with reinforcing steel in their cross-sectional profiles. The "Concrete07" material in OpenSees was implemented to simulate the behavior of confined and unconfined concrete. Moreover, the model proposed by Mander et al. [47] was utilized to represent the behavior of confined concrete. The modeling of cap beams, pile caps, and abutments involved employing elastic beam-column elements.

Elastomeric bearings were modeled using elastic-perfectly plastic materials with a friction coefficient of 0.4 following Caltrans [48]. Table 2 describes the main properties of elastomers used in the study. The vertical bearing stiffness is denoted by K_v, the pier elastomer's shear stiffness is indicated by K_s, and the shear stiffness of the abutments in the longitudinal and transverse directions are represented by K_{al} and K_{at}, respectively. The type of bridge utilized in this study is susceptible to potential poundings between discontinuous elements within their superstructure. To evaluate this behavior, the researchers employed zero-length elements with a bilinear behavioral model, as suggested by Muthukumar and DesRoches [49], which were positioned between the nodes of adjacent girders and girder-abutment connections.

Table 2
The characteristics of elastomer defined in this study

$K_s(\frac{kN}{mm})$	$K_{al}(\frac{kN}{mm})$	$K_{at}(\frac{kN}{mm})$	$K_v(\frac{kN}{mm})$
2.53	10.14	22.94	695

Two sets of matching points were used to model the behavior of the abutments and their backfills, which created matching surfaces. This study incorporated the hyperbolic force-deformation behavior of the abutment-backfill system by using compression-only nonlinear zero-length elements with Hyperbolic Gap

material characteristics as defined in OpenSees. Specifically, one end of each spring was attached to the corresponding node of a rigid grid creating the abutment surface, while the other end was fixed to nodes representing the backfill [50]. Shear keys were employed in bridge abutments to provide transverse support for superstructure movements under seismic loads. This was achieved by using zero-length elements with a nonlinear force-deformation behavior, according to the research of Megally et al. [51].Selecting a comprehensive method for modeling soil-structure interaction in studies within the field of scouring is of utmost importance. This study employed the p-y, t-z, and q-z springs at the soil-pile interface to simulate the lateral resistance, axial friction, and tip-bearing resistance, respectively. The load-deflection curve of the p-y springs was determined utilizing the methodology suggested by the American Petroleum Institute, with due consideration given to the sand properties [52]. The backbone of the t-z curve is approximated according to Mosher [53], using the calculated ultimate side friction axial resistance according to Kulhawy [54,55]. Also, the behavior of q-z material was modeled by Vijayvergiya's relation [56] for piles. In addition, the ultimate resistance of the pile tip (q_U) was calculated according to the Meyerhof method [57,58]. All the springs mentioned have been modeled utilizing zero-length elements in the foundation. The p-y and t-z springs in this study were spaced out at 0.25m intervals along the length of the pile. To account for scour-induced cavities, the corresponding springs at the soil-pile interface were removed. The geometric characteristics and the material behavior curves in the finite element model are depicted in Fig. 3.

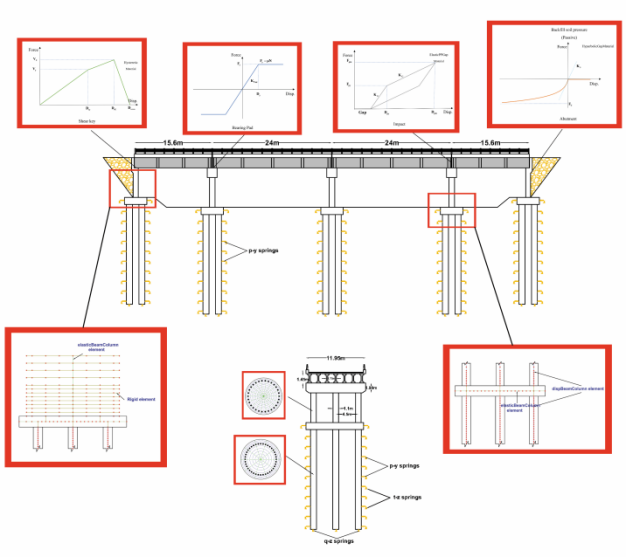

Fig. 3. Schematic illustration of the bridge

3.3. Response History Analysis

It is essential to examine the scouring patterns of the research model under seismic loads to assess the combined impact of the earthquake-scouring on the bridge structure. Thus, nonlinear response-history analyses (NRHA) were conducted to evaluate scoured models with various scenarios in this study. To accomplish this goal, a suite of 40 strong ground motions was chosen. The selected set of ground motions contains two distinct faulting mechanisms, including strike-slip and dip-slip. These seismic records were captured on soil profiles having shear wave velocities (v_{s30}) ranging from 175 to 375 m/s. Their moment magnitudes (M_W) fall within the range of 6 to 7.5. As presented in Tables 3 and 4, the chosen ground motions exhibit a vast range of peak ground acceleration (PGA) and encompass source-to-site distances varying from near-field to far-field earthquakes. It is worth mentioning that the selected near-fault earthquakes were of both pulse-like and non-pulse types. The seismic analyses were carried out in this study by randomly inducing the dominant horizontal component of the earthquake in either the longitudinal or transverse direction of the bridge.

Table 3
List of Dip-slip ground motions

Record	M_W	Year	PGA(g)	$v_{s30}(\frac{m}{s})$	R_{jb}(km)	R_{RUP}(km)
Taiwan Smart(45)-O07	7.3	1986	0.16	314.33	54.17	54.17
N.Palm Springs-Palm Springs Airport	6.1	1986	0.19	312.47	10.08	10.84
Loma Prieta-Capitola	6.9	1989	0.51	288.62	8.65	15.23
Tabas-Boshrooyeh	7.4	1978	0.11	324.57	24.07	28.79
Taiwan Smart(45)-I07	7.3	1986	0.12	309.41	55.82	55.82
Coalinga-Cantua Creek School	6.4	1983	0.29	274.73	23.78	24.02
Taiwan Smart(45)-C00	7.3	1986	0.15	309.41	56.01	56.01
Coalinga-Pleasant Valley	6.4	1983	0.60	257.38	7.69	8.41
Gazli-Karakyr	6.8	1976	0.86	259.59	3.92	5.46
N.Palm Springs-North Palm Springs	6.1	1986	0.69	344.67	0	4.04
Taiwan Smart(40)-E01	6.3	1986	0.21	308.39	55.96	57.25
Northridge-Newhall.Fire Sta	6.7	1994	0.59	269.14	3.16	5.92
Loma Prieta-Gilory Array#3	6.9	1989	0.56	349.85	12.23	12.82
Whittier Narrows-Whittier Narrows Dam Upstream	6.0	1987	0.32	298.68	2.6	14.73
Northridge-Sylmar.Converter Sta	6.7	1994	0.92	251.24	0	5.35
Whittier Narrows-Bell Gardens Jaboneria	6.0	1987	0.23	267.13	10.31	17.79
Northridge-Canoga Park.Topanga Can	6.7	1994	0.39	267.49	0	14.7
Chi Chi Taiwan03-TCU065	6.2	1999	0.35	305.85	25.17	26.05
Chi Chi Taiwan06-CHY036	6.3	1999	0.20	233.14	45.1	46.19
Northridge01-Tarzana-Cedar Hill A	6.7	1994	1.78	257.21	0.37	15.6

Table 4
List of Strike-slip ground motions

Record	M_W	Year	PGA(g)	$v_{s30}(\frac{m}{s})$	R_{jb}(km)	R_{RUP}(km)
Landers-Baker Fire Station	7.3	1992	0.11	324.62	87.94	87.94
Parkfield-Cholame Shandon Array#8	6.2	1966	0.27	256.82	12.9	12.9
Imperial Valley-Bonds Corner	6.5	1979	0.78	223.03	0.44	2.66
Trinidad-Rio Dell Overpass E Ground	7.2	1980	0.16	311.75	76.06	76.26
Chalfant Valley02-Bishop LADWP South St	6.2	1986	0.25	303.47	14.38	17.17
Parkfield 02 CA-Parkfield Fault Zone 1	6.0	2004	0.83	178.27	0.02	2.51
Morgan Hill-Hollister City Hall	6.2	1984	0.07	198.77	30.76	30.76
Imperial Valley06-Compuertas	6.5	1979	0.19	259.86	13.52	15.3
Darfield New Zealand-Kaiapoi North School	7.0	2010	0.36	255	30.53	30.53
Parkfield 02 CA-Parkfield Fault Zone 15	6.0	2004	0.23	307.59	0.8	2.67
Imperial Valley 06-El Centro Array #8	6.5	1979	0.61	206.08	3.86	3.86
Superstition Hills 02-Parachute Test Site	6.5	1987	0.43	348.69	0.95	0.95
Victoria Mexico-SAHOP Flores	6.3	1980	0.10	259.59	39.1	39.3
Morgan Hill-Gilory Array #4	6.2	1984	0.35	221.78	11.53	11.54
Parkfield 02 CA-Parkfield Cholame 2WA	6.0	2004	0.62	173.02	1.63	3.01
Parkfield-Cholame Shandon Array #5	6.2	1966	0.44	289.56	9.58	9.58
Parkfield 02 CA-Parkfield Cholame 3W	6.0	2004	0.58	230.57	2.55	3.63
Kocaeli-Yarimca	7.5	1999	0.32	297	1.38	4.83
Parkfield 02 CA-Parkfield Fault Zone 14	6.0	2004	1.31	246.07	8.45	8.81
Chalfant Valley-Zack Brothers Ranch	6.2	1986	0.45	316.19	6.44	7.58

Fig. 4 depicts a collection of response spectra that were obtained from the dominant component of ground motions, and additionally, the mean response spectrum has been computed.

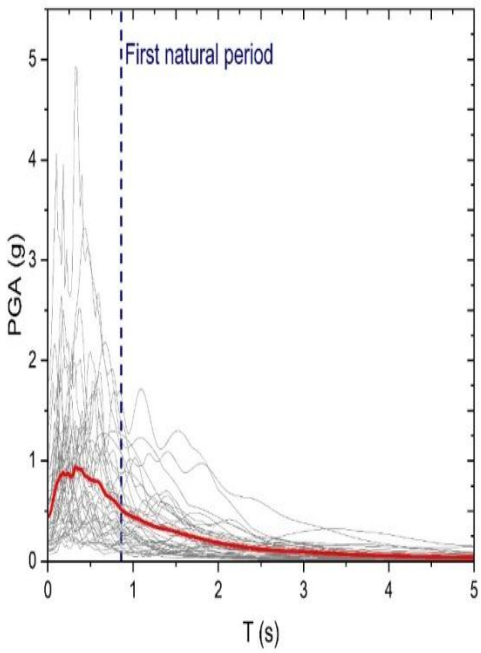

Fig. 4. Response spectra of the selected ground motions (5%damping)

4-Bridge Performance

A specific scouring scenario can have a notable impact on the performance and response of a structure to a particular excitation. Essentially, alterations in scouring patterns can impact the performance of a bridge by changing its support conditions along with its dynamic characteristics. The main objective of this study is to evaluate the behavior of the bridge structure under various scouring scenarios, namely intact, uniform scouring, non-uniform scouring, and uniformly maximum credible scouring (UMCS), using NRHA analysis. It is substantial to clarify that the term uniform in this context refers to bridges that experience the same random scour depth around all their foundations. On the other hand, the uniformly maximum credible scoured bridges are those that are exposed to the highest possible amount of uniform scouring within a selected return period. Furthermore, in bridges that

experience non-uniform scour, the scour depth of each pier is randomly assigned.

As investigating the behavior of bridges under non-uniform scour was one of the primary objectives of this study, this pattern has been categorized into several specific scouring forms based on the random generation of cavities around the different foundations. (See Table 5).

Table 5
Scouring form description

Scouring form	Description	Shape
Ramp shaped	The scour depth gradually increases from one side of the river cross section to its opposite side.	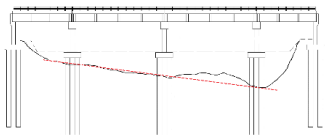
Step shaped	The scouring depth of the two adjacent bents are the same and differ from the other pier.	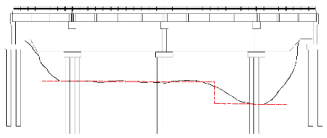
V-shaped	The scour depth of the middle bent is higher than the other ones.	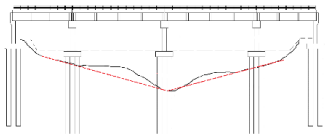
Λ-shaped	The scour depth of the middle bent is less than the other ones.	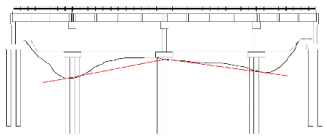

4.1. The Impact of Scouring Scenarios on the Maximum Base Shear Forces

The total maximum base shear values were derived from time history analyses of the models under various scour conditions. Fig. 5 displays the distribution of these results. The figure also depicts the minimum, maximum, and mean values in addition to a linear fit that illustrates the correlation between two sets of data.

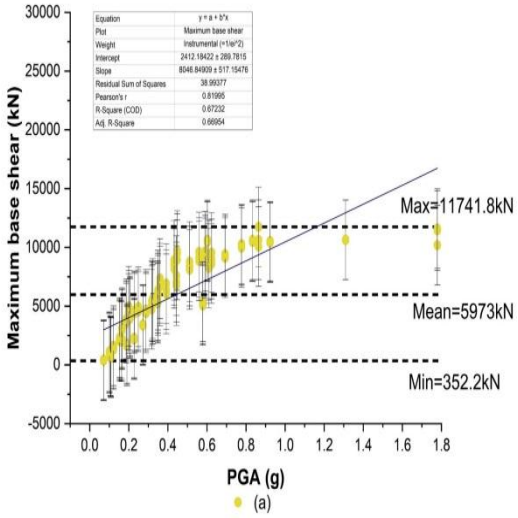

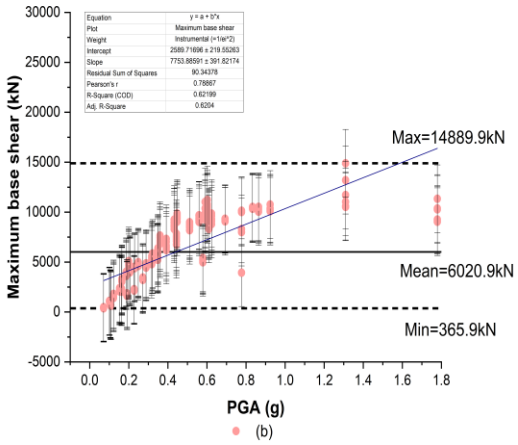

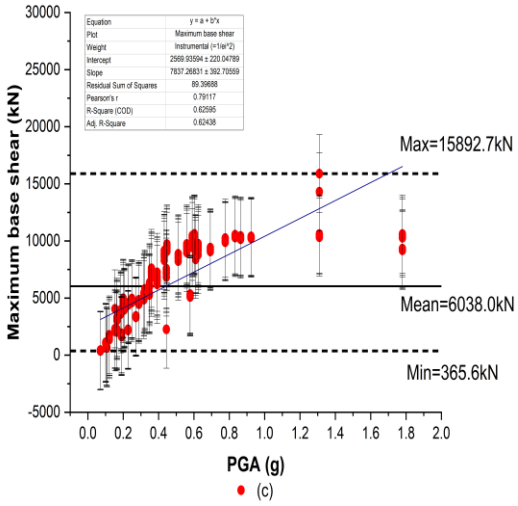

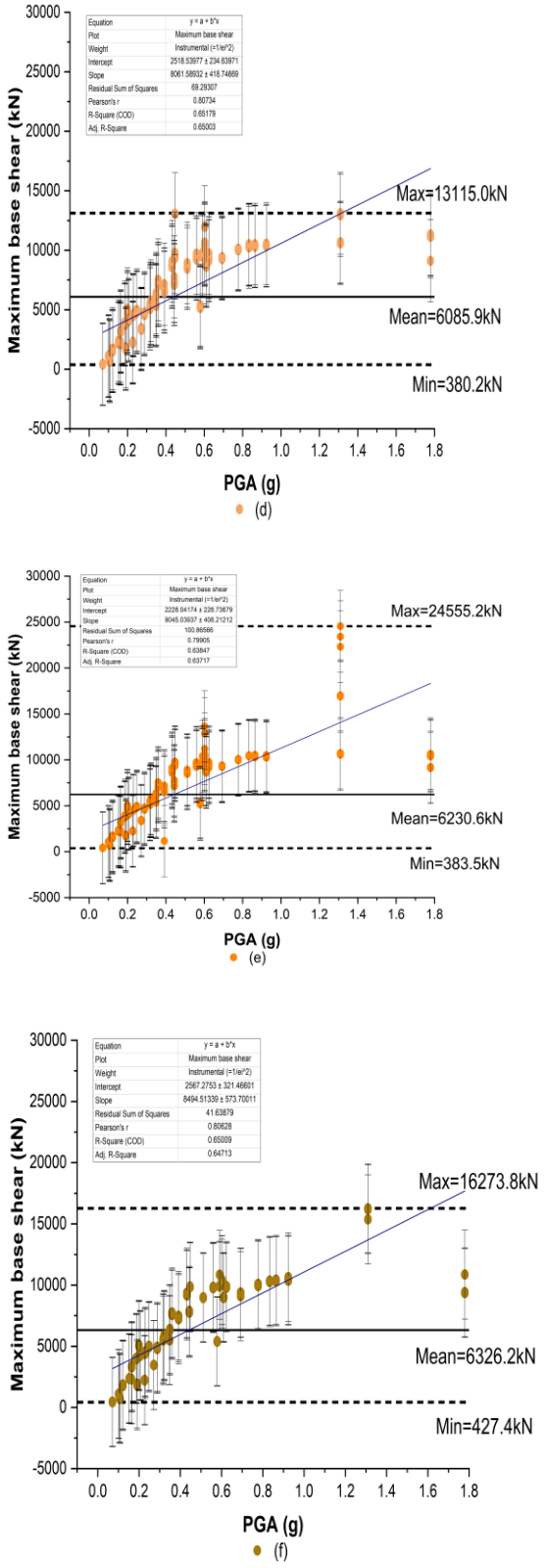

Fig. 5. Maximum base shear values recorded in models of (a) Intact (b) Ramp-shaped (c) Step-shaped (d) V-shaped (e) Λ-shaped (f) UMCS

The findings demonstrate that, among scouring forms, the Λ-shaped leads to the highest mean base shear force, whereas the ramp-shaped results in the lowest mean value. This finding agrees with the fragility analysis that indicated more susceptibility on the Λ-shaped scour form [30]. Table 6 presents the mean and standard deviation of the maximum base shear recorded for various scour scenarios. The minimum recorded mean value corresponds to the intact condition, while the highest value is associated with the UMCS scouring pattern. Notably, the uniform scouring pattern recorded a high mean value (higher than the non-uniform pattern), which is comparable to the recorded value for UMCS.

Table 6
Mean and standard deviation of recorded maximum base shear values for different scour scenarios

Scour scenario	Maximum base shear(kN)	
	Mean	Sd
Intact	5973.0	3387.7
Uniform	6291.7	3741.8
Non-uniform	6099.9	3556.1
UMCS	6326.2	3636.7

Overall, the recorded results suggest that foundation scouring leads to an increase in total base shear. The maximum mean base shear (MMBS) recorded in the uniform and UMCS patterns exhibit a growth rate of 5.3% and 6%, respectively, compared to the intact condition. Among the various non-uniform scouring forms, the Λ-shaped displays a 4.3% increase in the MMBS while little change in this parameter is observed in the other three forms.

4.2. Deck Displacement

The chosen ground motions consist of near-field records that exhibit pulse-like and non-pulse behaviors. The longitudinal and transverse deck displacements resulting from the Northridge-Newhall Fire Sta pulse-like record (PGA=0.59) and the Imperial Valley-Bonds Corner non-pulse record (PGA=0.78g) are illustrated in Fig. 6. The effect of scouring was examined using the UMCS pattern for both models. The findings indicate relatively large displacements that persisted as residuals in the longitudinal direction.

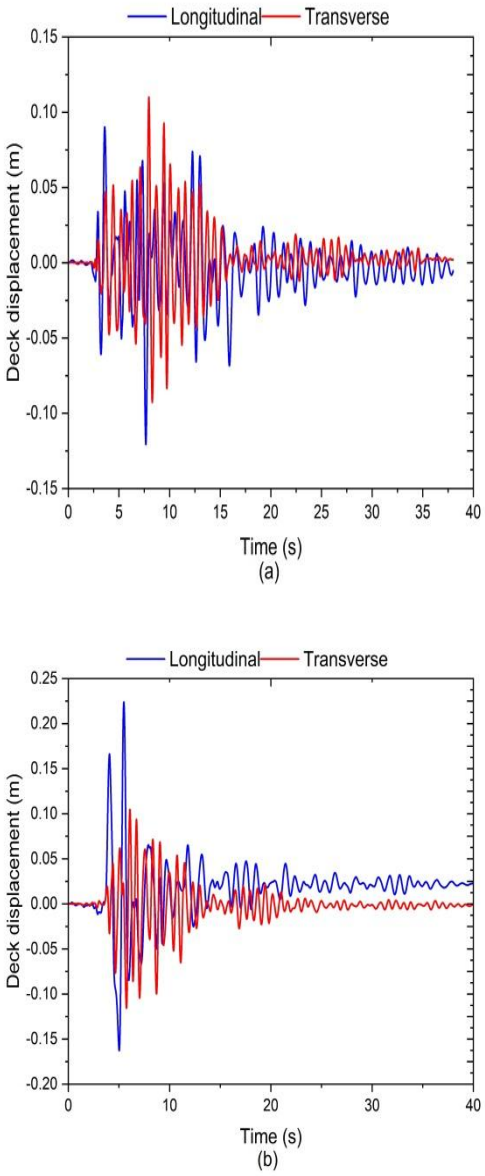

Fig. 6. The time history of the deck displacement for (a) Imperial Valley-Bonds Corner and (b) Northridge-Newhall.Fire Sta records

The comparison of the two records indicated that the pulse-like behavior of the Northridge earthquake resulted in a larger and permanent displacement in the longitudinal direction of the bridge despite having a smaller PGA.

4.3. The Impact of Scouring Scenarios on the Maximum Pounding Forces

Moderate to massive earthquake events may cause out-of-phase motion of the frames in a bridge due to variations in the dynamic characteristics of adjacent spans, ground motion variability, and propagation wave effects [59]. These different phase vibrations resulting from seismic events can cause collisions to occur between an abutment and girder, adjacent girders, or between a girder element and a neighboring structure [60]. Pounding-induced bridges have been observed during several earthquake events [61]. When pounding occurs, great forces can be generated in the impact zero-length elements within the bridge's finite-element model. To assess the influence of scouring scenarios on the intensity of impact force in earthquake analyses, Fig. 7 illustrates the overall count of observed pounding events and the force value recorded in a single girder for each corresponding case.

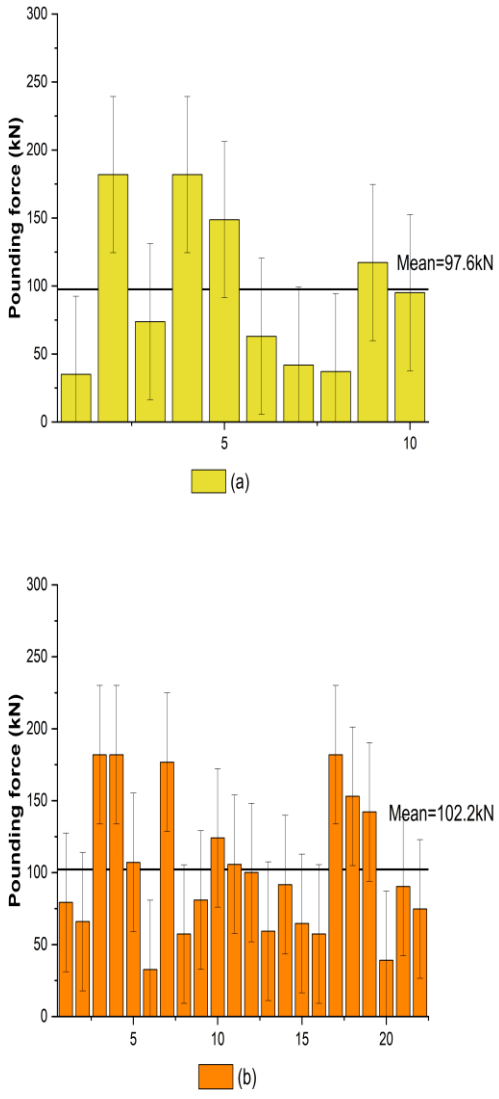

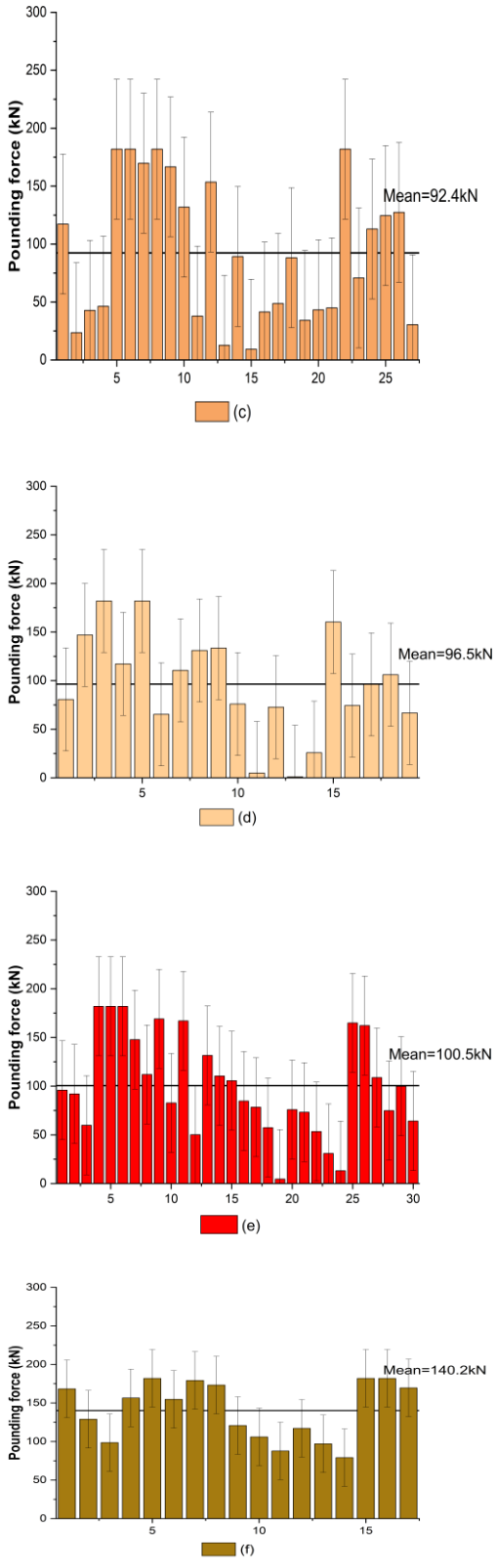

Fig. 7. Pounding force in a single girder for (a) Intact (b) Ramp-shaped (c) Step-shaped (d) V-shaped (e) Λ-shaped (f) UMCS

Table 7 listed the mean and standard deviation of pounding forces for different scouring conditions. The study's findings indicate that transitioning from the intact to UMCS pattern leads to a 44% rise in the mean pounding force. Furthermore, the uniform pattern has increased the mean load by roughly 11% compared to the intact. Based on the recorded data, the results indicate a relatively substantial rise in the applied pounding forces.

Table 7
Mean and standard deviation of recorded pounding force values for different scour scenarios

Scouring pattern	Pounding force(kN)	
	Mean	Sd
Intact	97.6	57.4
Uniform	108.1	50.0
Non-uniform	97.9	53.0
UMCS	140.2	37.3

While the non-uniform scouring pattern did not significantly increase mean pounding force, the ramp and Λ-shaped recorded 5% and 3% increases, respectively, compared to the intact condition.

4.4. Pile Performance

The assessment of foundation pile performance is essential due to the direct correlation between the behavior of these structural elements and the scouring. Any alteration or impairment of the foundation pile can lead to subsequent impacts on the functionality of other structural components that rely on pile stability. Hence, this study aimed to evaluate the performance of a single pile in three separate bent foundations. This assessment involved extracting maximum displacement, shear, moment, and lateral responses of p-y springs as soil responses at varying heights. Three seismic records were selected to represent non-pulse and pulse-like near-field and far-field earthquakes: Coalinga-Pleasant Valley (PGA=0.6g), Parkfield 02 CA- Parkfield Fault Zone 1 (PGA=0.83g), and Darfield New Zealand-Kaiapoi North School (PGA=0.36g). The performance of intact and UMCS bridge models was evaluated, along with four different forms of non-uniform scenarios. It is important to note that the performance of the different non-uniform models cannot be compared to one another since they were randomly selected. Fig. 8 illustrates the pile responses obtained from various seismic analyses.

As anticipated, higher scour depths lead to increased displacement, particularly in the pile cap. The shear force in the middle section of the pile and at the bottom of the scour cavity both increase as scour depth increases. Another important aspect is the linear reduction of the force across the washed-out zone. Despite this reduction, there is evidence to suggest that the shear force recorded in the pile cap is greater (albeit to a slight extent) than that in the intact model in a majority of cases. This phenomenon can be more distinctly observed in the results of far-field earthquake analysis, as depicted in Fig. 8 (c). The third bent of the ramp form was an exception because the scour depth was much less than the other two bents. It seems that the shear force was mainly directed towards the foundations of the two bents, leading to the shear force recorded in the pile cap of the third bent being slightly lower than that of the intact model. It is important to note that this issue needs further investigation and analysis.

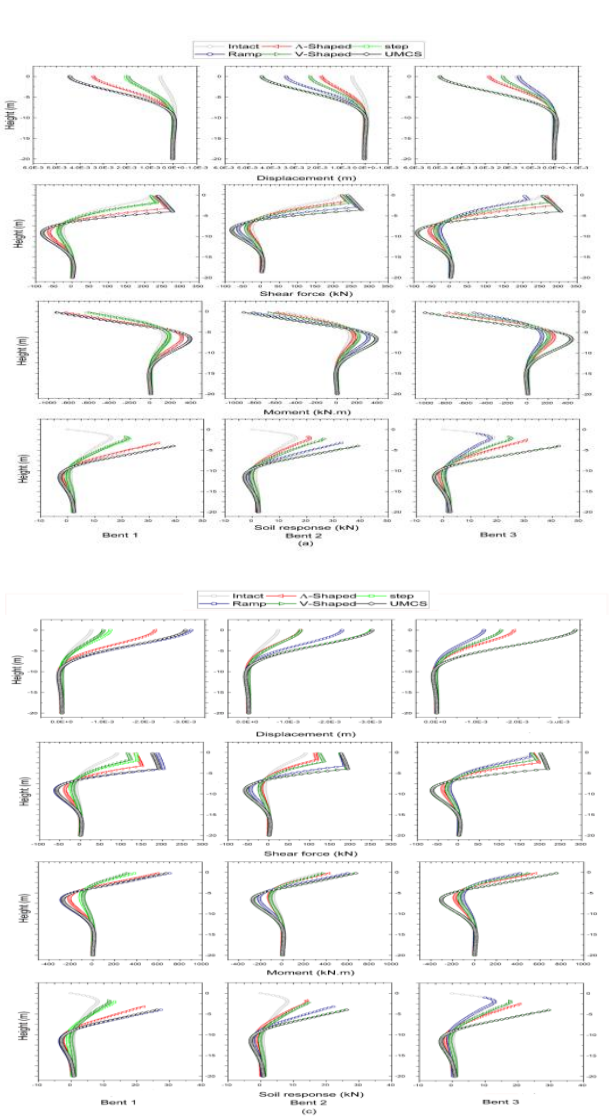

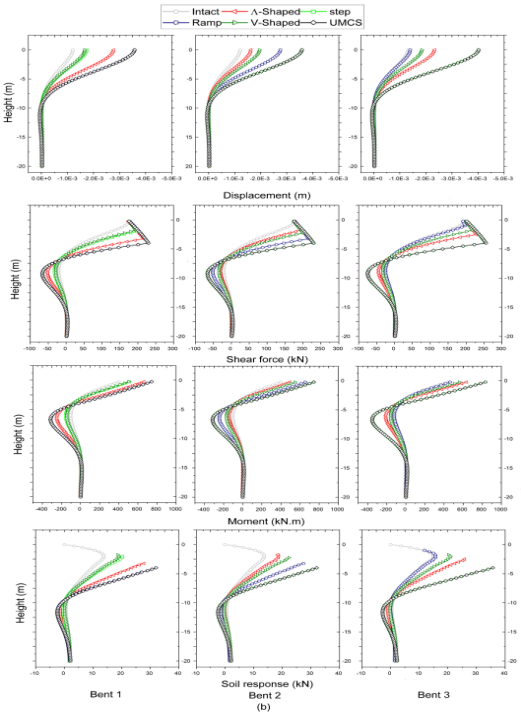

Fig. 8. Investigation of pile responses to different scour scenarios in seismic analyses of (a) Parkfield 02 CA- Parkfield Fault Zone 1 (PGA=0.83g) (b) Coalinga-Pleasant Valley (PGA=0.6g), and (c) Darfield New Zealand-Kaiapoi North School records

confirms that scour depth directly affects the soil responses, with the most marked responses, at the bottom of the washed-out zone for scenarios with deeper scouring. In models subjected to a depth of scour of 4 meters, the maximum soil responses occasionally exceed 2.3 times the highest response recorded in the intact condition.Furthermore, the findings indicate that scenarios with deeper scour depths result in larger moments at the pile cap, as well as in an area comprising roughly one-third of the pile height. Moreover, the analysis confirms that scour depth directly affects the soil responses, with the most marked responses, at the bottom of the washed-out zone for scenarios with deeper scouring. In models subjected to a depth of scour of 4 meters, the maximum soil responses occasionally exceed 2.3 times the highest response recorded in the intact condition.the pile height. Moreover, the analysis confirms that scour depth directly affects the soil responses, with the most marked responses, at the bottom of the washed-out zone for scenarios with deeper scouring. In models subjected to a depth of scour of 4 meters, the maximum soil responses occasionally exceed 2.3 times the highest response recorded in the intact condition.

5-Conclusions

In this study, a randomized evaluation was conducted to assess the impact of scouring around the foundations of various bents in a multi-span bridge. The researchers employed a probabilistic framework that utilized Monte Carlo simulation to estimate the probabilistic scour hazard curve. Furthermore, random scouring depths were generated in different bents using the Latin .Hypercube Sampling technique. Scouring scenarios in bridge foundations were classified into four categories: intact, uniform, non-uniform, and uniform maximum credible scour pattern (UMCS).After conducting non-linear seismic analyses based on selected seismic records for the scouring scenarios, the researchers determined the bridge responses. This study also divided the non-uniform scouring scenario into multiple forms and evaluated the effect of each scoured model on the total base shear and girder pounding force.Based on the performance analyses conducted on the bridge structure under different scouring scenarios, it has been observed that the mean maximum base shear (MMBS) value for the intact model is lower compared to the non-uniform and uniform scenarios. The UMCS pattern has resulted in the highest MMBS value among all the scouring patterns.The findings reveal a 2.1%, 5.3%, and 6% increase in the MMBS value for the non-uniform, uniform, and UMCS scenarios, respectively, compared to the intact condition. Additionally, the Λ-shaped scouring form has led to a 4.3% increase in the MMBS value as compared to the intact scenario.The analyses of pounding force between the girders reveal that transitioning from the intact condition to the uniform and the UMCS patterns leads to an increase of 11% and 44% in the mean pounding forces, respectively. Although the non-uniform scenario has not resulted in a significant increase in the mean pounding force, it has been found that the ramp and Λ-shaped scour forms have led to an increase of 5% and 3%, respectively, in the mean pounding forces compared to the intact condition.The results of the performance assessment of piles based on some samples of seismic analyses indicate an increase in responses under different scour scenarios. The change in displacement and soil responses, as well as variations in shear and moment along the pile height, display an increment in most cases with the increase in scour depth. Scouring significantly increases the soil response and the shear force at the bottom of the washed-out zone. It also causes higher values of moment and displacement in the pile cap.The findings of this study indicate that scour scenarios exert a noticeable influence on the performance of the bridge model. Notwithstanding, these results are specific to the particular model that this study examined. To phrase it differently, alterations in the bridge's classification, component geometry, material characteristics, or other pertinent factors could produce different results. Therefore, it is crucial to conduct a meticulous analysis before endeavoring to generalize these findings.

References

[1] Shirole, A. M., Holt, R. C. (1991). Planning for a comprehensive bridge safety assurance program. Transportation Research Record, 1290, 39-50.

[2] Richardson, E. V., HUBER, F. W. (1991). Evaluation of Bridge Vulnerability to Hydraulic Forces, Stream Instability. Transportation Research Record, 1290, 25.

[3] Lagasse, P. F. (1997). Instrumentation for measuring scour at bridge piers and abutments (No. 21). Transportation Research Board.

[4] Kwak, K. (2001). Prediction of scour depth versus time for bridge piers in the case of multi-flood and multi-layer soil system. KSCE Journal of Civil Engineering, 5, 67-74.

[5] Khan, K. A., Muzzammil, M., Alam, J. (2016). Bridge Pier Scour: A review of mechanism, causes and geotechnical aspects. Proc. Adv. Geotech. Eng, 8-9.

[6] Wardhana, K., Hadipriono, F. C. (2003). Analysis of recent bridge failures in the United States. Journal of performance of constructed facilities, 17(3), 144-150.

[7] Hayes, D. C., Drummond, F. E. (1995). Use of fathometers and electrical-conductivity probes to monitor riverbed scour at bridge piers (Vol. 94, No. 4164). US Department of the Interior, US Geological Survey.

[8] Yankielun, N. E., Zabilansky, L. (1999). Laboratory investigation of time-domain reflectometry system for monitoring bridge scour. Journal of Hydraulic engineering, 125(12), 1279-1284.

[9] Hunt, B. E. 2009. Monitoring scour critical bridges: a synthesis of highway practice. Synthesis of highway practice, 396.

[10] AASHTO (American Association of State Highway and Transportation Officials). (2020). LRFD Bridge Design Specifications, 9th ed. AASHTO LRFDBDS-9(2020). Washington, DC:

[11] Wang, Z., Padgett, J. E., Dueñas-Osorio, L. (2014). Risk-consistent calibration of load factors for the design of reinforced concrete bridges under the combined effects of earthquake and scour hazards. Engineering Structures, 79, 86-95.

[12] Priestley, M. J. N. (1988). The Whittier narrows, California earthquake of October 1, 1987—Damage to the I-5/I-605 separator. Earthquake Spectra, 4(2), 389-405.

[13] Mitchell, D., Bruneau, M., Saatcioglu, M., Williams, M., Anderson, D., Sexsmith, R. (1995). Performance of bridges in the 1994 Northridge earthquake. Canadian Journal of Civil Engineering, 22(2), 415-427.

[14] Chang, K.C., Chang, D. W., Tsai, M. H., Sung Y. C. (2000). Seismic Performance of Highway Bridges.

[15] Di Sarno, L., Da Porto, F., Guerrini, G., Calvi, P. M., Camata, G., Prota, A. (2019). Seismic performance of bridges during the 2016 Central Italy earthquakes. Bulletin of Earthquake Engineering, 17, 5729-5761.

[16] Nielson, B. G., DesRoches, R. (2007). Seismic performance assessment of simply supported and continuous multispan concrete girder highway bridges. Journal of Bridge Engineering, 12(5), 611-620.

[17] Erhan, S., Dicleli, M. (2015). Comparative assessment of the seismic performance of integral and conventional bridges with respect to the differences at the abutments. Bulletin of Earthquake Engineering, 13, 653-677.

Vulnerability, uncertainty, and risk: Analysis, modeling, and management (pp. 889-896).

[18] Sha, B., Tao, T., Xing, C., Wang, H., Li, A. (2020). Pounding analysis of isolated girder bridge under nonpulse and pulse-like earthquakes. Journal of Performance of Constructed Facilities, 34(4), 04020062.

[19] Kameshwar, S., Padgett, J. E. (2018). Response and fragility assessment of bridge columns subjected to barge-bridge collision and scour. Engineering Structures, 168, 308-319.

[20] Hung, C. C., Yau, W. G. (2014). Behavior of scoured bridge piers subjected to flood-induced loads. Engineering Structures, 80, 241-250.

[21] Prendergast, L. J., Gavin, K. (2014). A review of bridge scour monitoring techniques. Journal of Rock Mechanics and Geotechnical Engineering, 6(2), 138-149.

[22] Banerjee, S., Prasad, G. G. (2011). Analysis of bridge performance under the combined effect of earthquake and flood-induced scour. In

[23] Alipour A., Shafei, B., Shinozuka, M. (2013). Reliability-based calibration of load and resistance factors for design of RC bridges under multiple extreme events: Scour and earthquake. Journal of Bridge Engineering, 18(5), 362-371.

[24] He, H., Wei, K., Zhang, J., Qin, S. (2020). Application of endurance time method to seismic fragility evaluation of highway bridges considering scour effect. Soil Dynamics and Earthquake Engineering, 136, 106243.

[25] Ren, J., Song, J., Ellingwood, B. R. (2021). Reliability assessment framework of deteriorating reinforced concrete bridges subjected to earthquake and pier scour. Engineering Structures, 239, 112363.

[26] Song, S. T., Hu, T. F., Chiou, D. J. (2022). Influence of riverbed scour on the performance of bridges subjected to lateral seismic loads. Journal of Earthquake Engineering, 26(5), 2251-2282.

[27] He, L. G., Hung, H. H., Chuang, C. Y., Huang, C. W. (2020). Seismic assessments for scoured bridges with pile foundations. Engineering Structures, 211, 110454.

[28] Shrestha, A., Shrestha, B., Sahani, K. (2023). Seismic Response of RC Bridge considering scour effect: A Case Study of Kathmandu Valley. ce/papers, 6(5), 1295-1302.

[29] Fioklou, A., Alipour, A. (2019). Significance of non-uniform scour on the seismic performance of bridges. Structure and Infrastructure Engineering, 15(6), 822-836.

[30] Hosseini, A. R. M., Razzaghi, M. S., Shamskia, N. (2023). Probabilistic seismic safety assessment of bridges with random pier scouring. Proceedings of the Institution of Civil Engineers-Structures and Buildings, 1-18.

[31] Neil, C. R. (1964). River bed scour, a review for bridge engineers. Contract No. 281. Research Council of Alberta, Calgary, Alta., Canada.

[32] Melville, B. W., Sutherland, A. J. (1988). Design method for local scour at bridge piers. Journal of Hydraulic Engineering, 114(10), 1210-1226.

[33] Froehlich, D. C. (1988). Analysis of onsite measurements of scour at piers. In Hydraulic engineering: proceedings of the 1988 national conference on hydraulic engineering (pp. 534-539).

[34] Richardson, E. V., Davis S. R. (1995). Evaluating scour at bridges (No. HEC 18). United States. Federal Highway Administration. Office of Technology Applications.

[35] Melville, B. W. (1997). Pier and abutment scour: integrated approach. Journal of hydraulic Engineering, 123(2), 125-136.

[36] Sheppard, D. M., Odeh, M., Glasser, T. (2004). Large scale clear-water local pier scour experiments. Journal of Hydraulic Engineering, 130(10), 957-963.

[37] Coleman, S. E. (2005). Clearwater local scour at complex piers. Journal of Hydraulic Engineering, 131(4), 330-334.

[38] Kothyari, U. C., Hager, W. H., Oliveto, G. (2007). Generalized approach for clear-water scour at bridge foundation elements. Journal of hydraulic Engineering, 133(11), 1229-1240.

[39] Lança, R. M., Fael, C. S., Maia, R. J., Pêgo, J. P., Cardoso, A. H. (2013). Clear-water scour at comparatively large cylindrical piers. Journal of Hydraulic Engineering, 139(11), 1117-1125.

[40] Yang, Y., Melville, B. W., Macky, G. H., Shamseldin, A. Y. (2019). Local scour at complex bridge piers in close proximity under clear-water and live-bed flow regime. Water, 11(8), 1530.

[41] Johnson, P. A., Dock, D. A. (1998). Probabilistic bridge scour estimates. Journal of Hydraulic Engineering, 124(7), 750-754.

[42] Bolduc, L. C., Gardoni, P., Briaud, J. L. (2008). Probability of exceedance estimates for scour depth around bridge piers. Journal of Geotechnical and Geoenvironmental Engineering, 134(2), 175-184.

[43] Bolduc, L. C. (2010). Probabilistic models and reliability analysis of scour depth around bridge piers. (Doctoral dissertation, Texas A & M University).

[44] Alipour, A., Shafei, B. (2012). Performance assessment of highway bridges under earthquake and scour effects. In Proceedings of the 15th world conference on earthquake engineering (pp. 24-28).

[45] Mosleh, A., Sepahvand, K., Varum, H., Jara, J., Razzaghi, M. S., Marburg, S. (2018). Stochastic collocation-based nonlinear analysis of concrete bridges with uncertain parameters. Structure and Infrastructure Engineering, 14(10), 1324-1338.

[46] Mazzoni, S., McKenna, F., Scott, M. H., Fenves, G. L. (2006). Open system for earthquake engineering simulation user command-language manual. Pacific Earthquake Engineering Research Center, University of California, Berkeley, OpenSees version, 1(3).

[47] Mander, J. B., Priestley, M. J., Park, R. (1988). Theoretical stress-strain model for confined concrete. Journal of structural engineering, 114(8), 1804-1826.

[48] CALTRANS (2004). Seismic design criteria. Version 1.3, California Dept. of Transportation, Sacramento, CA.

[49] Muthukumar, S., DesRoches, R. (2006). A Hertz contact model with non- linear damping for pounding simulation. Earthquake engineering & structural dynamics, 35(7), 811-828.

[50] Simon, J., Vigh, L. G. (2016). Seismic fragility assessment of integral precast multi-span bridges

in areas of moderate seismicity. Bulletin of Earthquake Engineering, 14, 3125-3150.

[51] Megally, S. H., Silva, P. F., Seible, F. (2001). Seismic response of sacrificial shear keys in bridge abutments. SSRP, 23.

[52] API (American Petroleum Institute). (1993). Recommended practice for planning, designing, and constructing fixed offshore platforms, working stress design, 20th ed. Washington, D.C, American Petroleum Institute.

[53] Mosher, R. L. (1984). Load-Transfer Criteria for Numerical Analysis of Axially Loaded Piles in Sand. Part 1. Load-Transfer Criteria. ARMY ENGINEER WATERWAYS EXPERIMENT STATION VICKSBURG MS.

[54] Kulhawy, F. H. (1991). Drilled Shaft Foundations, Chapter 14 in Foundation Engineering Handbook, H.-Y. Fang, Editor.

[55] Zhang, L., Silva, F., Grismala, R. (2005). Ultimate lateral resistance to piles in cohesionless soils. Journal of Geotechnical and Geoenvironmental Engineering, 131(1), 78-83.

[56] Vijayvergiya, V. N. (1977). Load-movement characteristics of piles. In 4th Symp. of Waterway, Port, Coastal and Occean Div., ASCE (Vol. 2, pp. 269-284).

[57] Meyerhof, G. G. (1976). Bearing capacity and settlement of pile foundations. Journal of the Geotechnical Engineering Division, 102(3), 197-228.

[58] Das, B. M., and Sivakugan, N. (2018). Principles of foundation engineering. Cengage learning.

[59] DesRoches, R., Muthukumar, S. (2002). Effect of pounding and restrainers on seismic response of multiple-frame bridges. Journal of Structural Engineering, 128(7), 860-869.

[60] Jankowski, R., Wilde, K., Fujino, Y. (1998). Pounding of superstructure segments in isolated elevated bridge during earthquakes. Earthquake engineering & structural dynamics, 27(5), 487-502.

[61] Miari, M., Choong, K. K., Jankowski, R. (2021). Seismic pounding between bridge segments: a state-of-the-art review. Archives of Computational Methods in Engineering, 28, 495-504.